Proceedings of the 14th International Plansee Seminar, Eds. G. Kneringer, P. Rödhammer and P. Wilhartitz, Plansee AG, Reutte (1997), Vol. 1

Mo COATINGS PRODUCED WITH THE AID OF THE VACUUM ARC DEPOSITION

B.B.Straumal[1-3], V.G.Glebovsky[1], N.F.Vershinin[1,3], V.G.Sursaeva[1], W.Gust[2]

[1]Institute of Solid State Physics, Chernogolovka, Moscow District 142432 Russia
[2]Institut für Metallkunde, Seestr. 75, D-70174 Stuttgart, Germany
[3]Institute for Vacuum Technology (IVT Ltd.), Chajanov str. 8/26, Moscow, 125047 Russia

ZUSAMMENFASSUNG:

Die Herstellung von Mo-Beschichtungen oder dünnen Folien ist anhand der Vakuumlichtbogenabscheidung möglich. Die Verdampfung des Kathodenmaterials während der Vakuumlichtbogenentladung läßt hohe Abscheidungrate erreichen, die unabhängig vom Zerstäubungskoeffizienten des Targets sind. Die Abscheidungsrate, die Rauhigkeit, die Oberflächenmorphologie und das Gefüge der Mo-Schichten wurden in Abhängigkeit von der Abscheidungsdauer, des Entladungsstroms und dem Abstand von der Kathode untersucht. Es wurden hohe Abscheidungsraten von 15 nm/s erreicht. Die Möglichkeiten, wie man die Rauhiget, das Gefüge und die Adhesion der Mo-Beschichtung gezielt kontrollieren kann, werden dargestellt.

SUMMARY:

The manufacturing of Mo in form of coatings or foils is possible with the aid of vacuum arc deposition. The evaporation of the target in the arc discharge, which burns in the vapour of the cathode material itself, permits one to reach high deposition rates independently on the sputter coefficient of the target. The deposition rate, the roughness, the surface morphology and the microstructure of the Mo coatings on different substrates have been studied in dependence on the deposition time, the current and the distance from the cathode. Deposition rates of 15 nm/s have been reached. The possibility to control the roughness, the microstructure and the adhesion of thin and thick Mo coatings has been demonstrated.
KEYWORDS: Mo coatings, vacuum arc deposition, microparticles

Proceedings of the 14th International Plansee Seminar, Eds. G. Kneringer, P. Rödhammer and P. Wilhartitz, Plansee AG, Reutte (1997), Vol. 1

INTRODUCTION

Refractory metals are widely used in modern technology due to their exceptional properties, particularly to the hardness and high stability against corrosive media (1). Most hard metal components are currently made by traditional powder metallurgy techniques such as die pressing followed by sintering. This process not only limits the complexity of the parts which can be produced, but as the components are produced entirely from hard metal they are, therefore, expensive and brittle. However, in many applications the bulk characteristics of a refractory metal are not used and only the specific mechanical or protective properties of a rather thin surface layer are important. In such cases the proper coating technology permits one to use the one material like a steel to fabricate a base structure of the product (like cutting tool) and a refractory metal is utilised to form the cutting or protective surfaces. In this manner the best properties of both materials can be exploited. This would result not only in significant cost saving coming from the reduced level of hard metal utilisation but would give an enhanced degree of toughness, higher durability and improvement of component life.

Various processes are now used for production of hard and refractive coatings like chemical vapour deposition (2), molten salt electrodeposition (3), magnetron deposition (4, 5). Unfortunately, these methods have important disadvantages. Therefore, a flexible and universal technology for production of rather thick dense multicomponent refractory coatings on the complex parts should de found.

One of the good candidates is the vacuum arc deposition. This technology firstly invented in 60s (6) is now widely used for production of hard TiN or diamond-like coatings (7–9). The vacuum arc deposition has important potentialities which make this technology very promising for various applications. One advantage is the high deposition rate of metals like Mo which can be achieved (10). The arc discharge burns in the vapour of the cathode material itself. The target material evaporates and is ionized in this discharge. Therefore, the deposition rate do not depend on the sputter coefficient (7). It makes the sputtering rate high and practically independent on the type of the cathode material. Other expected advantage of the vacuum arc process lie in the increased flexibility in size and the complexity of parts which can be produced. The low deposition temperature (generally below 100°C) permits one to deposit the coatings even on the

substrates sensible to overheating (like polymers). The interesting peculiarity of vacuum arc deposition most important for its application is the possibility for changing the properties of the substrate surface and growing film with the aid of a combined flux of multiply charged ions and microparticles. It is widely believed that microparticles have a deteriorating effect on the properties of the deposited layers (11). However, in many applications the roughness of the film caused by the incorporated microparticles has either no effect or can be even useful.

The deposition of Mo coatings is an important technological problem. For example, Mo–Al coatings were recently developed for a combined corrosion protection against oxidation and sulphurization (4, 5). However, the sputter coefficient of Mo is low, and this circumstance makes difficult the magnetron deposition of Mo (12). In this work the vacuum arc deposition of Mo on different substrates is studied. The dependence of the deposition rate, roughness and morphology of the Mo layer on the discharge current, the distance between substrate and cathode and their mutual orientation was investigated.

EXPERIMENTAL

Mo coatings have been deposited onto polished Cu and silica glass substrates in a vacuum arc apparatus described elsewhere (10). The pumping system of the apparatus consists of a Balzers turbomolecular pump with a capacity of 1500 ℓ/s and two rotary pumps with a total capacity of 40 ℓ/s. The pressure during deposition is 8×10^{-4} Pa. The vacuum chamber has the form of a horizontal cylinder of 700 mm diameter and 500 mm length. At the end of this cylinder the vacuum arc apparatus with the magnetic system for spot stabilization and the Mo cathode are placed. The cathode of diameter D = 60 mm was made from 99.95% Mo. It was prepared by high-vacuum electron-beam multiple melting in specially designed water-cooled copper moulds (13). The facilities for magnetic filtering of the macroparticles were not used in this study. The substrates were placed in different distances L from the surface of the cathode (L = 50, 175, 300 and 425 mm). At each distance the substrates were positioned parallel (θ = 0°) and perpendicular (θ = 90°) to the plasma flow coming axially from the cathode (θ is the angle between the direction of the plasma flow and the surface of the substrate). The vacuum arc source voltage was constant U = 31 V, and the discharge current was changed (I = 80, 100,

140 and 180 A). The strength of the stabilizing magnetic field on the cathode surface was 60 to 70 G. No bias has been applied to the substrates. The coating time was changed (t = 5, 10, 20 and 40 min). In order to avoid an overheating of the substrates the coating process was interrupted without breaking a vacuum every 2.5 min for 2.5 to 3 min.

The thickness of the coatings d was measured with the aid of a profilometer and an optical microscope. With the aid of a polystep profilometer the height of a step was measured between the coated and protected halves of the substrate with an accuracy of 5 nm. The thickness of coatings with $d > 1$ μm was additionally measured with the aid of an optical microscope. The deposition rate was determined as mean value for four deposition times. The size of the microparticles was measured with the aid of a scanning electron microscope (JEOL 6400) and a Zeiss Axiophot optical microscope possessing contrast accessories which allow a resolution as low as 0.2 to 0.4 mm. The area S occupied by individual particles was determined to be $S = \pi r^2$ for round particles and $S = \pi ab/4$ for elliptical particles, where r is the radius, and a and b are the axes of the ellipse. The fractional coverage, $\Sigma S/S_t$, was determined to be the ratio of the total area of all particles counted, ΣS, to the total projected area on the substrate for all analysed rectangles S_t ($S_t = nS_C$, where S_C is the square of one counting area and n is the number of the rectangles counted). The roughness R_A was measured with the aid of a Sloan Dektak II profilometer and determined using the standard software. R_A was determined on two length scales, namely R_{A1000} for 1000 μm and R_{A50} for 50 μm. For each sample studied, R_A was measured in the direction perpendicular to the direction of the plasma flow 5 times at the length scale of 1000 μm and 20 to 30 times on the length scale of 50 μm.

RESULTS AND DISCUSSION

Figure 1 displays the surface morphology of Mo coatings deposited under various conditions. The substrates in Fig. 1a and c were placed perpendicular to the plasma flow. The substrates in Fig. 1b and d were placed parallel to the plasma flow. The morphology of the microparticles clearly differs for these two cases. The samples shown in Fig. 1a and b were placed closer to the cathode than those shown in Fig. 1c and d. The number of microparticles clearly decreases with increasing distance L. The coatings shown in Fig. 1b and d were deposited four times longer than those shown

Proceedings of the 14th International Plansee Seminar, Eds. G. Kneringer, P. Rödhammer and P. Wilhartitz, Plansee AG, Reutte (1997), Vol. 1

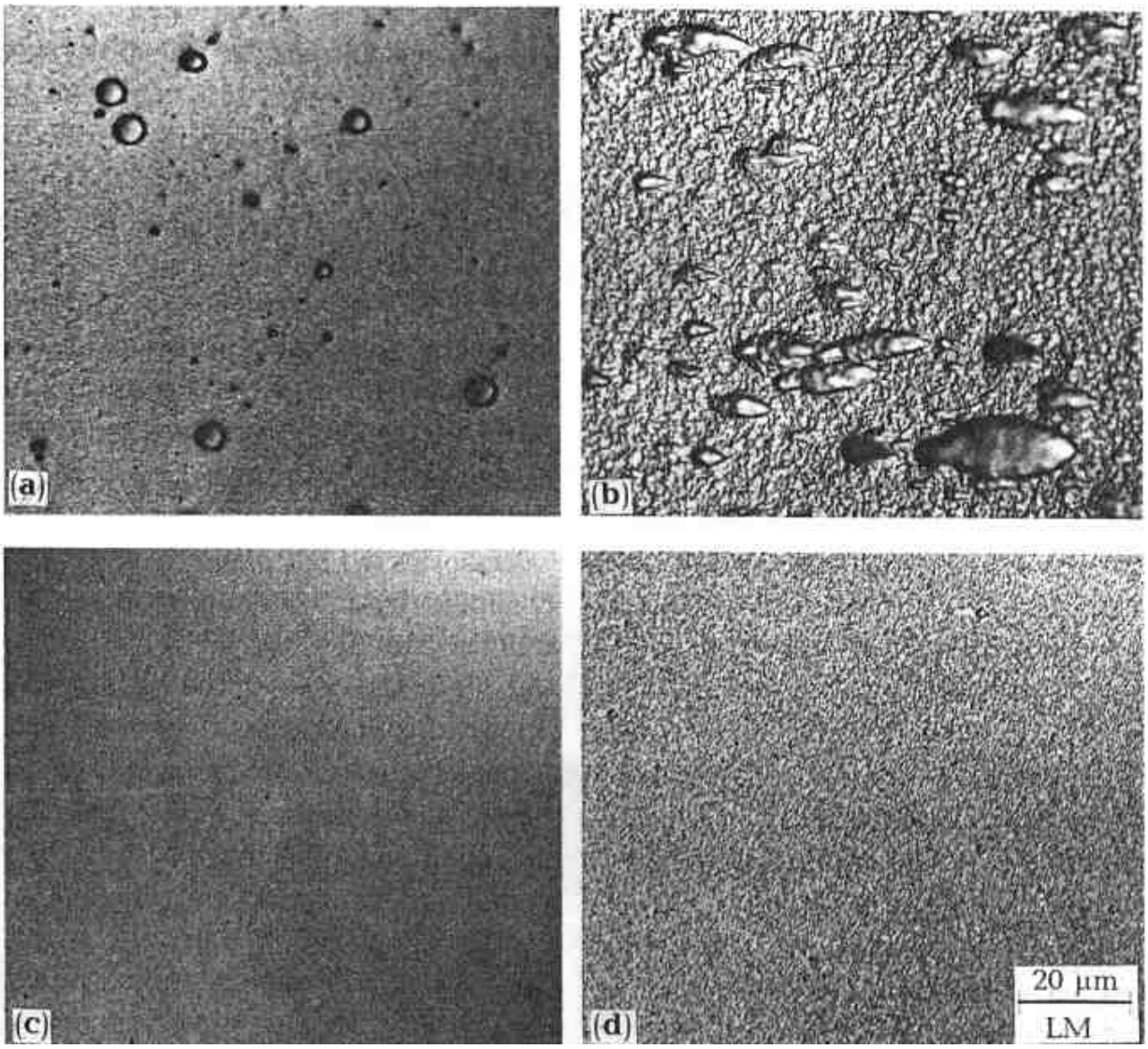

Fig. 1. Optical micrographs of the microstructure of Mo coatings. **(a)** Mo/glass, $\theta = 90°$, $I = 100$ A, $L = 50$ mm, $t = 5$ min; **(b)** Mo/glass, $\theta = 0°$, $I = 100$ A, $L = 50$ mm, $t = 20$ min; **(c)** Mo/glass, $\theta = 90°$, $I = 100$ A, $L = 300$ mm, $t = 5$ min; **(d)** Mo/glass, $\theta = 0°$, $I = 100$ A, $L = 175$ mm, $t = 20$ min.

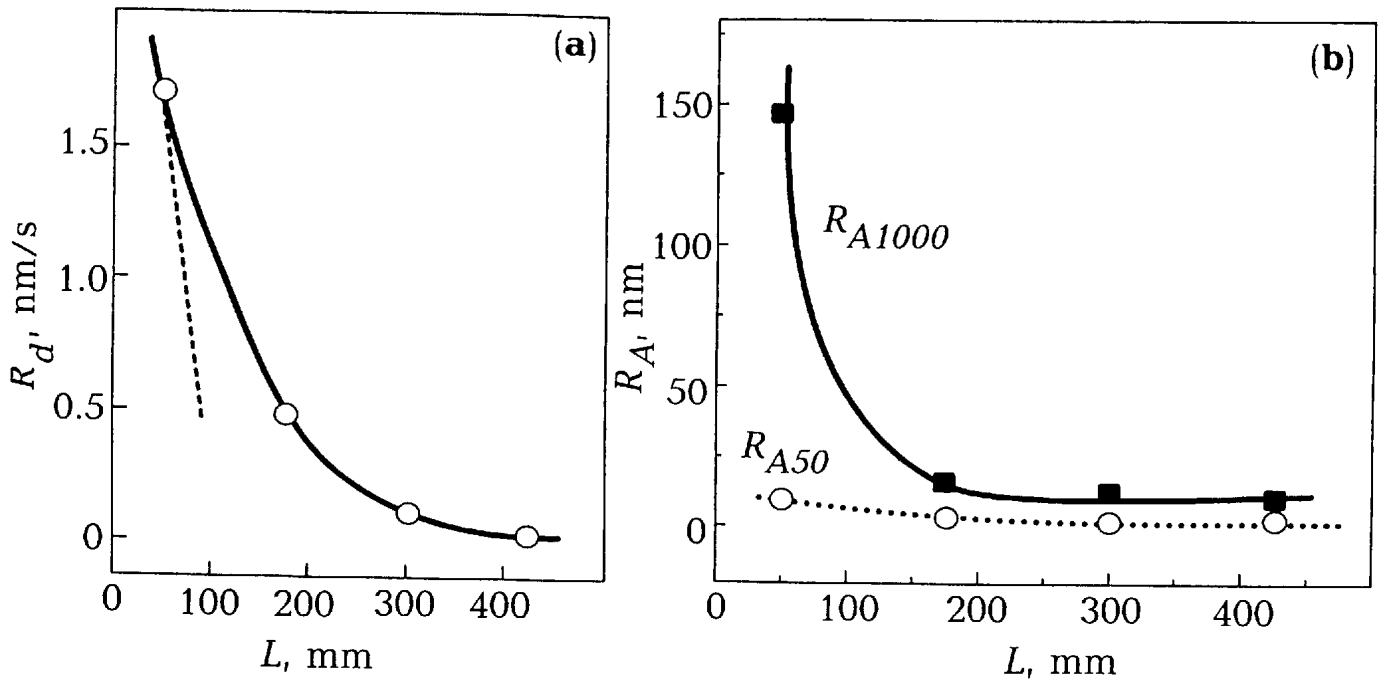

Fig. 2. Dependence of the deposition rate R_d **(a)** and of the roughness values R_{A1000} and R_{A50} **(b)** on the distance L between substrate and cathode for Mo films on Cu substrates. $\theta = 0°$, $I = 100$ A, $t = 5$ min.

in the Fig. 1a and c. The roughness of the coatings definitely increases with increasing deposition time t and decreasing L.

In Fig. 2a the dependence of the deposition rate R_d is shown on the distance L between cathode and substrate for substrates oriented parallel to the plasma flow coming from the cathode for a discharge power $P = 3.1$ kW. For $\theta = 0°$ at $L = 50$ mm the value $R_d = 15$ nm/s has been reached (10). The broken line shows the slope of the R_d (L) dependence for the Mo magnetron sputter deposition taken from (12) for the same discharge power and comparable L/D ratios, D being the diameter of the cathode. Normally, only the R_d values for $L/D < 1$ can be found in the literature for the magnetron sputter deposition, because reasonable deposition rates can be reached only if the substrates are positioned close to the target. If the distance L exceeds the diameter of the magnetic ring behind the target the deposition rate decreases with increasing L even faster as it is shown in Fig. 2a. It is obvious that R_d for vacuum arc deposition decreases with increasing L *much slower than in the case of magnetron sputter deposition.* It can be also clearly seen that the vacuum arc deposition permits to obtain R_d values which are *higher than R_d values reached with the aid of magnetron sputter deposition*

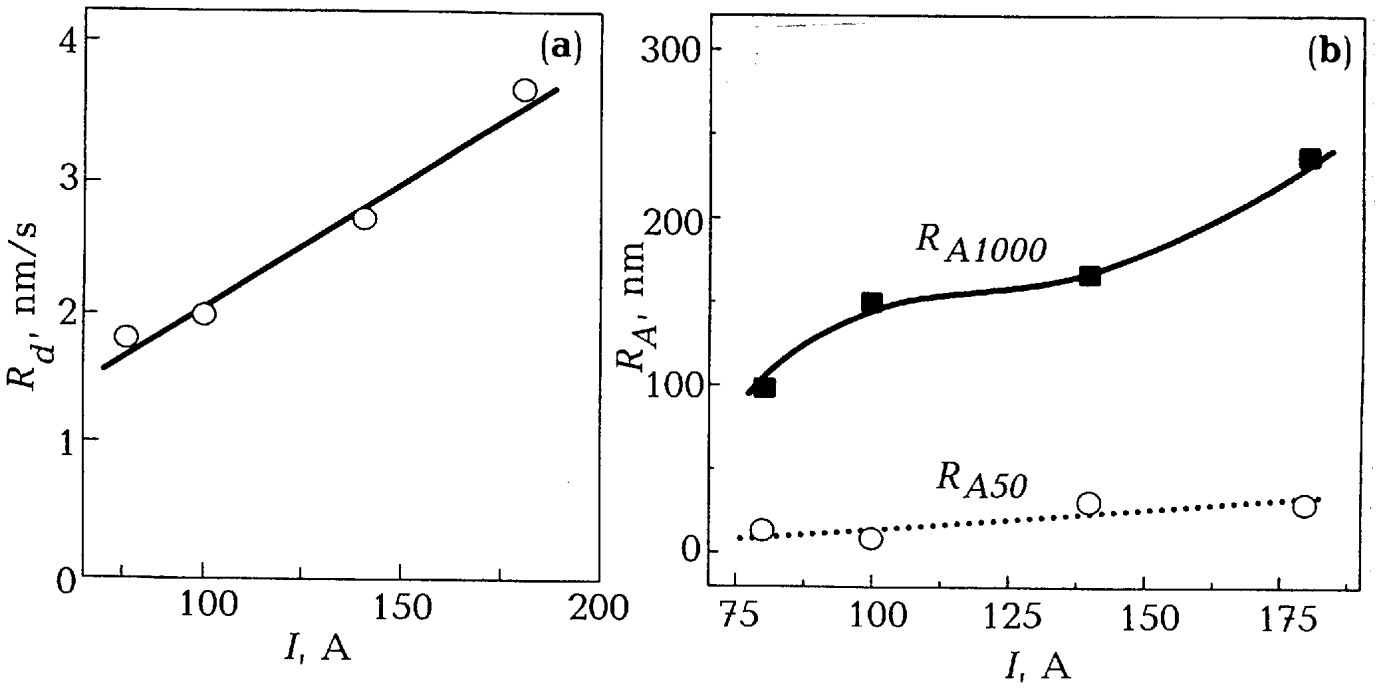

Fig. 3. Dependence of the deposition rate R_d **(a)** and of the roughness values R_{A1000} and R_{A50} **(b)** on the discharge current I for Mo films on Cu substrates. $\theta = 0°$, $L = 50$ mm, $t = 5$ min.

at the same values of P, L/D and θ. The R_d values on the substrates perpendicular to the plasma flow ($\theta = 90°$) are higher than for $\theta = 0°$ (10). But this difference decreases with increasing L/D (10). A slow decrease of R_d with increasing L/D and comparable values for normal and tangential incidence make easy *the coating of non-planar and three-dimensional parts with the aid of vacuum arc deposition.* Figure 3a shows the dependence of the deposition rate R_d on the discharge current I. The deposition rate increases almost linearly with increasing discharge current.

Numerous theoretical and experimental studies show that the roughness of the growing coatings depends strongly on the deposition process and can be described with the aid of fractal models (14). The roughness depends principally on the length of the measurement path and increases with increasing length scale (14, 15). The microparticles in the coating can influence drastically the roughness. Therefore, the roughness was measured on two length scales for each sample studied, namely 1000 and 50 μm. The measurements on the 1000 μm scale should characterize the overall roughness of the sample including the microparticles. The positions

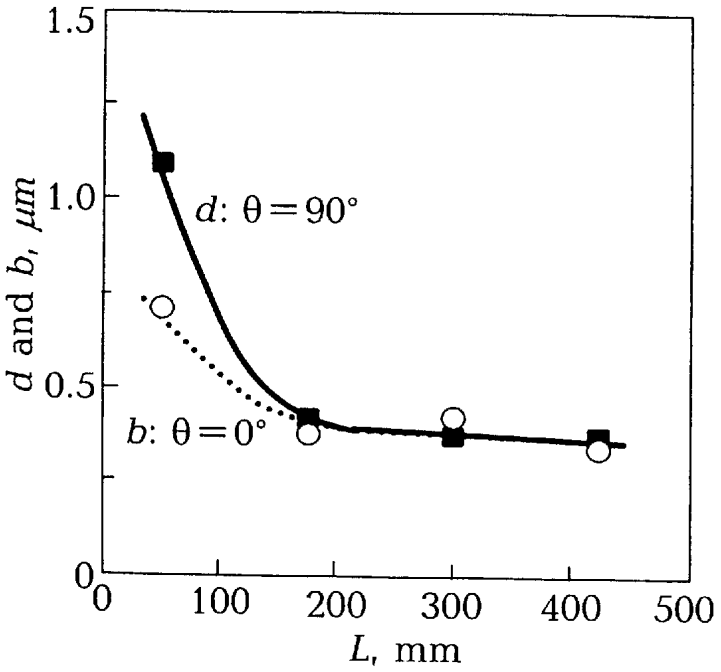

Fig. 4. Dependence of the diameter d (for normal incidence $\theta = 90°$) and the width b (for tangential incidence $\theta = 0°$) of individual droplets on the distance between substrate and cathode L. Mo/glass, $I = 100$ A, $t = 5$ min.

for the measurements on the 50 μm length scale were chosen mostly between the large particles. These data describe the roughness of the coating formed due to the condensation of ions without the influence of the particles, at least at low coating times t when the area coated by particles is low and the overlapping of the particles is negligible. In Fig. 2b the dependence of R_{A1000} and R_{A50} on the distance L is shown. For a low deposition time a bimodal roughness is present: individual particles can be clearly determined on the rather smooth background (see also the migrographs in Fig 1a and b). It can be supposed that the roughness of the coating between the microparticles is controlled mainly by the ion bombardment. The roughness of the background R_{A50} measured between the microparticles practically does not depend on L (Fig. 2b) and is below 10 nm. This value is comparable with the roughness of ion-bombarded surfaces (15). The measurements on the hillside of the extra large particles gave R_A values comparable with the R_A values at the 50 mm scale on a flat surface. The values of R_{A50} coincide with the grain size measured by transmission electron microscopy (16). It can be, therefore, concluded that R_{A50} is defined by smooth circular caps of individual grains.

The R_{A1000} values for $\theta = 0°$ are always higher than for $\theta = 90°$ (16). At the same time, the mean area of the individual particles for $\theta = 0°$ is lower than for $\theta = 90°$ (Fig. 4). Therefore, the particles on the substrates positioned parallel to the plasma flow are more flat than on the substrates

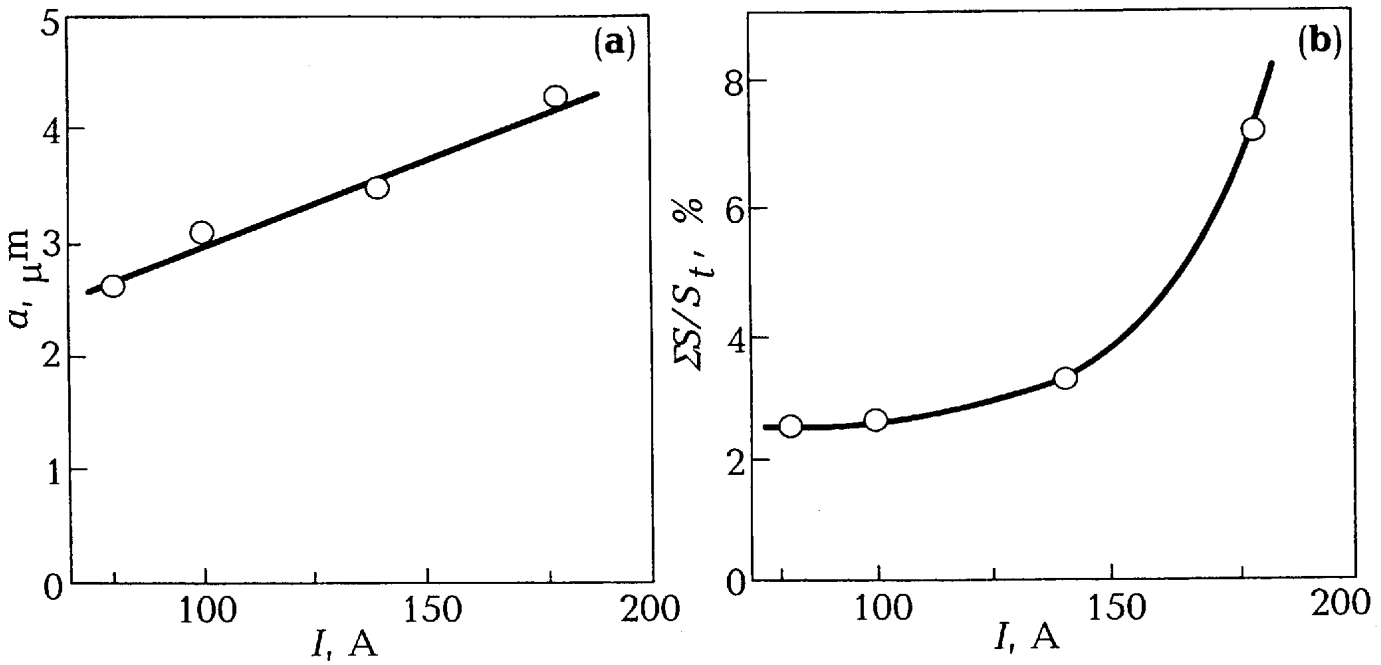

Fig. 5. Dependence of the mean length of the droplets a (**a**) and fractional coverage $\Sigma S/S_t$ (**b**) on the discharge current I. Mo/glass, L = 50 mm, θ = 0°, t = 5 min.

positioned perpendicular to the plasma flow. R_{A1000} decreases with increasing L both for $\theta = 0°$ and $\theta = 90°$ (16). It correlates with a decrease of the number and size of the microparticles with increasing L (Fig. 1 and 4). At low t, the increase of the discharge current I leads to an increase of R_{A1000} but does not influence R_{A50} (Fig. 3b). The behaviour of R_{A1000} can be explained by the increase of both the number and size of the microparticles with increasing I (Fig. 5). On the other hand, at t = 5 min the particles practically do not overlap for any I values studied (compare Figs. 1a and b). Therefore, the R_{A50} value does not exceed 30 nm and is not affected by a change of the discharge current.

The number, morphology and orientation of the microparticles deposited on the substrate are controlled by (a) the processes of their formation on the cathode in the vacuum arc spot, (b) the conditions of their flight in the electromagnetic field close to the source, (c) the conditions of their flight in the supersonic plasma flow close to the substrate, and (d) the collisions with the substrate.

The most important parameter influencing the formation of the microparticles on the cathode in the vacuum arc spot is the discharge

Proceedings of the 14th International Plansee Seminar, Eds. G. Kneringer, P. Rödhammer and P. Wilhartitz, Plansee AG, Reutte (1997), Vol. 1

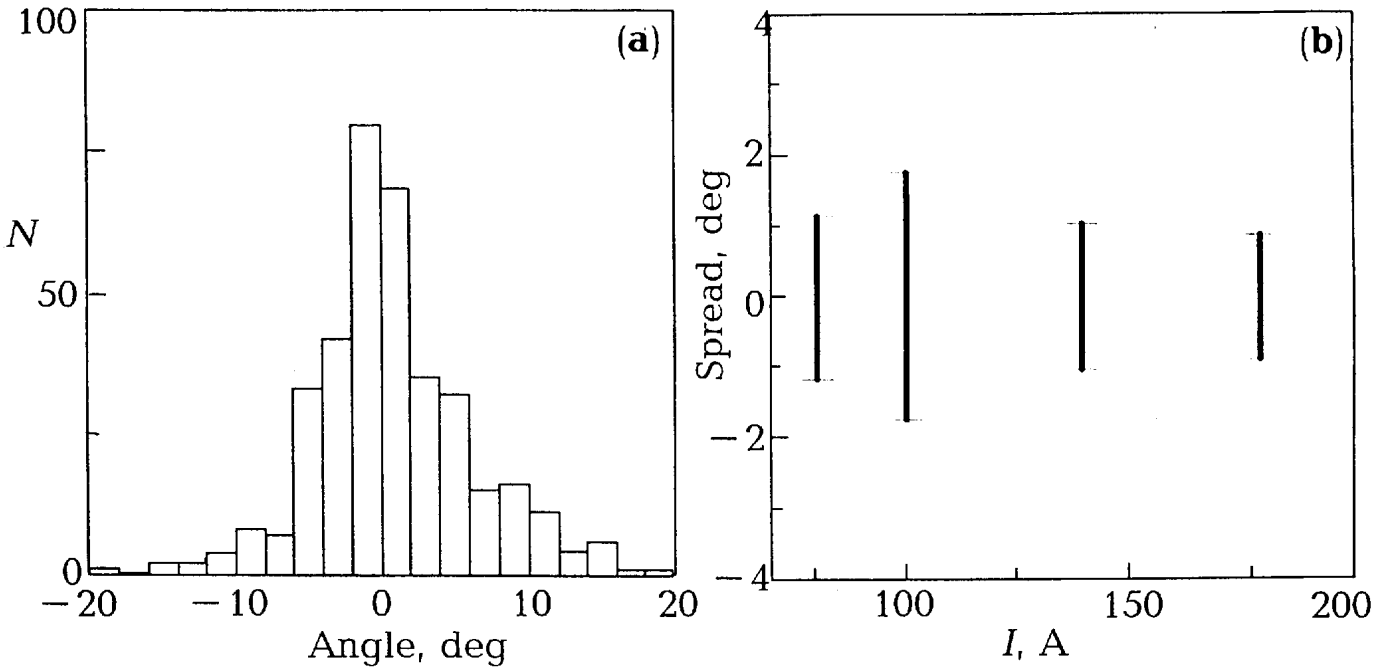

Fig. 6. **(a)** Angular distribution around the axis of the vacuum chamber for the elongated droplets at $\theta = 0°$ (I = 80 A). **(b)** Mean square spread of the angular distributions for different values of the discharge current I. Mo/glass, L = 50 mm, t = 5 min.

current I. Figure 5 displays the dependence of the mean length of the droplets a and of the fractional coverage $\Sigma S/S_t$ on I. The mean length of the droplets a increases linearly with increasing I (Fig. 5a). The fractional coverage increases parabolically with increasing I (Fig. 5b). The comparison of Figs. 3a and 5b definitely shows that R_d increases with increasing I slower than the fractional coverage. Therefore, *the contribution of the particles to the total deposition rate increases with increasing discharge current.* This fact can be explained by the increase of the cathode temperature with increasing I because it is known that an increase of the cathode temperature makes easier the formation of microdroplets in the cathode spot (7).

Figure 1 displays the morphology of microdroplets on the substrates positioned perpendicular (Fig. 1a and c) and parallel (Fig. 1b and d) to the plasma flow coming from the cathode. In the first case all droplets on the substrate are round. In the second case they have the form of ellipses elongated in the direction of the flight. The long axes of all droplets are nearly parallel to each other. Their angular distribution is rather narrow

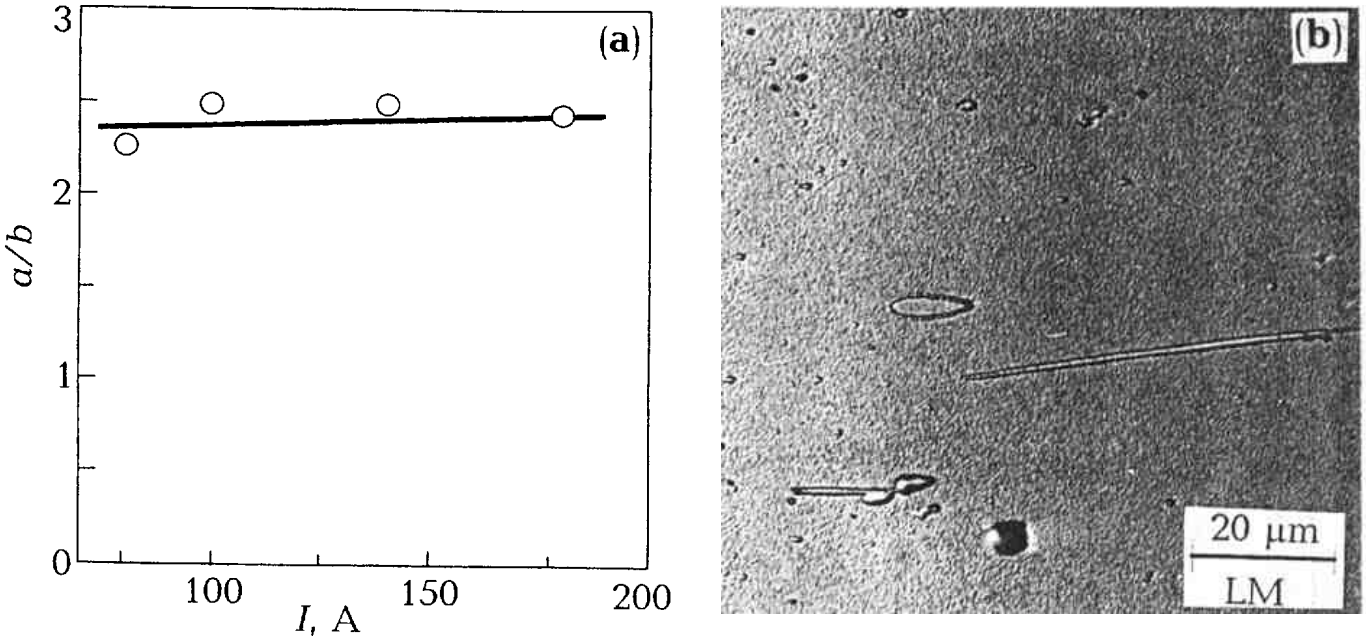

Fig. 7. (**a**) Dependence of the aspect ration a/b of individual droplets on the discharge current I for tangential incidence $\theta = 0°$. Mo/glass, L = 50 mm, t = 5 min. (b) Morphology of variuos microparticles. Mo/glass, L = 50 mm, I = 80 A, t = 5 min.

(Fig. 6a) and practically does not influenced by the discharge current I (Fig. 6b). Therefore, these parameters of the microparticles are controlled by the conditions of their flight in the plasma flow. Close to the cathode (L = 50 mm) the mean diameter, d, of round particles on the substrates positioned perpendicular to the plasma flow is lower than the mean width, b, of elliptical particles on the substrates positioned parallel to the plasma flow (Fig. 4). With increasing L the values d and b become smaller. They decrease to the greatest degree between L = 50 mm and L = 175 mm (Fig. 4, compare also Figs. 1a and b with Figs. 1c and d). Therefore, the *microparticles gradually disappear from the plasma flow with increasing time of flight* (or L). The coatings at $L > 50$ mm are almost free of particles (Fig. 1b and d). The possible mechanisms of their disappearance can be evaporation, sputtering by the Mo ions in plasma flow or fragmentation. The real mechanism can be determined by studying the time dependence of the size distributions of particles (17).

With increasing discharge current I the size of the microparticles formed also increases, though the aspect ratio a/b close to the cathode

Proceedings of the 14th International Plansee Seminar, Eds. G. Kneringer, P. Rödhammer and P. Wilhartitz, Plansee AG, Reutte (1997), Vol. 1

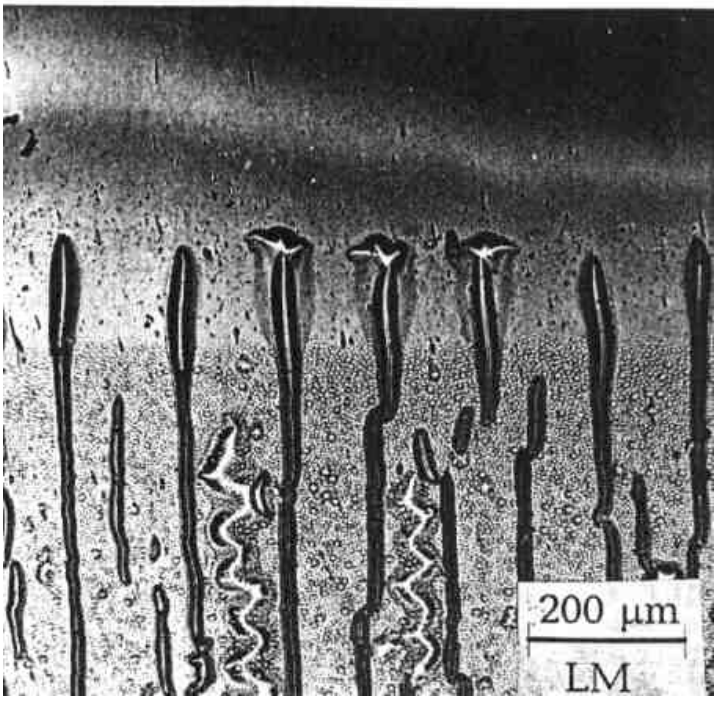

Fig. 8. Delamination of the coating close to the step between the protected and opened halves of the silica glass substrate. Mo/glass, L = 50 mm, I = 80 A, t = 5 min.

(L = 50 mm) is nearly constant for different values of I and is about 2.5 (Fig. 7a). The long microparticles (Fig. 7b) can be seen only seldom. Therefore, the sizes of the particles are controlled by their formation process in the arc spot, while their form in the coating is controlled by the conditions in the plasma flow close to the substrate and by the sticking conditions. Consequently, these conditions are nearly independent on the discharge current. The fractional coverage $\Sigma S/S_t$ increases nonlinearly with increasing I (Fig. 5b). The most important increase of $\Sigma S/S_t$ (from 0.03 to 0.07) occurs at high currents (between 140 and 180 A). At low deposition times t the particles cover only a minor part of the substrate surface (0.02 to 0.07 even at L = 50 mm) and do not overlap. With increasing deposition time, the particles are gradually incorporated into the coating, overlap each other and loose their "individuality", especially close to the cathode (compare Figs. 1a and b). Because of this, the measurement of the sizes of individual particles was possible only for t = 5 min. Only after short t the spontaneous detachment of some large particles can be seen (Fig. 7b). From the extrapolation the total area of the substrate can be covered with particles after about 1 h (at I = 180 A and L = 50 mm).

The size of the carbon particles in the vacuum arc deposited coatings (0.26 to 1.1 mm) obtained at L/D = 5.9 (18) is comparable with the results of our experiments: the size of the Mo particles is 0.7 to 1.8 mm for L/D = 0.83. The number density of the Mo particles in the case of normal

incidence (0.02 for L/D = 0.83 and 0.002 for L/D = 6.7) is much lower than that for carbon: 0.03 to 0.08 for L/D = 5.9 (18).

The adhesion of the studied Mo coatings depends on the substrate and the thickness of the coating. No bias was used in this study. It is known that applying the bias voltage one can change (normally, enhance) the adhesion of film to the substrate (11). In the same conditions all coatings on Cu substrate do not show any signs of delamination. The adhesion of Mo coatings to the silica glass is poorer. At d about 0.5 to 1.0 mm the internal stresses in the coating begin to exceed the adhesion force and spontaneous delamination starts (19). Figure 8 illustrates this delamination close to the step between the protected and opened halves of the silica glass substrate. The thickness of the coating gradually increases coming from the protected (upper part of the picture) to the unprotected half of the substrate. At certain d the coating begins to delaminate. For $d > 5$ mm the coatings on silica glass are practically totally delaminated (19). This feature can be in principle used for the manufacturing of thin Mo foils. For this purpose, another substrates instead of silica glass can be used with a lower adhesion, like for example fluoroplast. In the case of lower adhesion a spontaneous delamination can be reached for films with a thickness even lower than 1 μm.

We are thankful to Prof. Y. Brechet and Prof. T. Watanabe for stimulating discussions. The financial support from the INTAS programme under contract 93-1451 and TRANSFORM programm of the German Federal Ministry for Education, Science, Research and Technology (contract BMBF 03N9004) is acknowledged. One of us (B.S.) wish to thank the Heiwa Nakajima Foundation for the support of his stay at the Tohoku University where this paper was prepared.

REFERENCES

1. R. E. Smallwood, ed.: Refractory Metals and Their Industrial Applications, ASTM, Philadelphia, PA (1984) pp. 106–114.
2. F. A. Glaski: US Patent 3 767 456 (1973).
3. F. Cardarelli, P. Taxil and A. Savall: Int. J. Refractory Metals & Hard Materials 14 (1996) pp. 365–381.
4. K. Hashimoto P.-Y. Park, J.-H. Kim, H. Yoshioka, H. Mitzui, E. Akiyama, H. Hobazahi, A. Kawashi and K. Asami: Mat. Sci. Eng. A 196 (1995) pp. 1–10.

5. K.-L. Lin, Y.-J. Ho and J.-K.Ho: Thin Solid Films 263 (1995) pp. 85–91.
6. A. A. Plyutto, V. N. Ryzhkov and A. T. Kapin: Sov. Phys. JETP 20 (1965) pp. 328–337.
7. R. L. Boxman, P. J. Martin and D. M. Sanders, eds.: Handbook of Vacuum Arc Science and Technology, Noyes Publications, Park Ridge, NJ (1995) pp. 467–551.
8. L. P. Sablev: US Patent 3 783 231 (1974), US Patent 3 793 179 (1974).
9. N. F.Vershinin, A. M. Dorodnov and A. N. Kuznetzov: USSR Patent 1 292 552 (1985).
10. N. F. Vershinin, B. B. Straumal and W. Gust: J. Vac. Sci. Technol. A 14 (1996) pp. 3252–3255.
11. A. Anders, S. Anders, I. G. Brown, M. R. Dickinson and R. A. MacGill: J. Vac. Sci. Technol. B 12 (1994) pp. 815–820.
12. B. S. Danilin and V. K. Syrchin: Magnetron Sputtering Systems, Radio i svjas', Moscow (1982) pp.12–41 (in Russian).
13. V. G. Glebovsky, B. M. Shipilevsky, I. V. Kapchenko and V. V. Kyreiko: J. Alloys & Compounds 184 (1992) pp. 297–304.
14. J. Krim, I. Heyvaert, C. van Haesendonck and Y. Bruynseraede: Phys. Rev. Lett. 70 (1993) pp. 57–60.
15. G. S. Bales, R. Bruinsma, E. A. Eklund, R. P. Karunasiri, J. Rudnick and A. Zangwill: Science, 249 (1990) pp. 264–267.
16. B. Straumal, N. Vershinin, V. Semenov, V. Sursaeva and W. Gust: Defect Diff. Forum, in press.
17. Y. Brechet, private communication (1996).
18. M. Kandah and J.-L. Meunier: J. Vac. Sci. Technol. A 13 (1995) pp. 2444–2450.
19. N. F. Vershinin, V. G. Glebovsky, B. B. Straumal, W. Gust and H. Brongersma: Appl. Surf. Sci., in press.